(activity II/III). Elution with pentane–ether (3:1) yielded acetoxy ketone **6** (520 mg, 78.4%; ≥95% pure by ^{13}C NMR): mp 56–57 °C; ^{13}C NMR ($CDCl_3$) δ 216.1 (s), 169.8 (s), 79.5 (d), 52.6 (d), 46.4 (d), 45.7 (t), 41.5 (d), 39.4 (t), 36.5 (t), 34.1 (d), 21.1 (q); ^1H NMR ($CDCl_3$) δ 4.81 (s, 1 H), 2.9–1.8 (m, 13 H, maximum at δ 2.00); IR (KBr) 2945, 2870, 1740, 1240, 1230, 1215, 1065, 1025 cm^{-1}; MS, *m/z* (relative intensity) 194 (M^+, 6), 152 (21), 134 (5), 80 (100), 79 (25), 73 (21). Anal. Calcd for $C_{11}H_{14}O_3$: C, 68.02; H, 7.26. Found: C, 68.19; H, 6.98.

8-*exo*-Hydroxy-2-noradamantanone (7). A mixture of **6** (242 mg, 1.25 mmol), 50% aqueous methanol (15 mL), and potassium hydroxide (175 mg, 3.12 mmol) was stirred for 3 h at room temperature. The resulting mixture was saturated with sodium chloride and extracted with chloroform (3 × 30 mL). The extracts were combined and dried ($MgSO_4$). Evaporation of the solvent yielded hydroxy ketone **7** (180 mg, 94.7%; ≥95% pure by ^{13}C NMR): mp 248–250 °C; ^{13}C NMR ($CDCl_3$) δ 219.7 (s), 77.0 (d), 55.2 (d), 46.3 (d), 45.4 (t), 44.0 (d), 38.8 (t), 36.2 (t), 33.9 (d); ^1H NMR ($CDCl_3$) δ 3.92 (s, 1 H), 3.66 (br s, 1 H), 2.8–1.6 (m, 10 H, maximum at δ 1.80); IR (KBr) 3400, 2940, 2860, 1750, 1445, 1070, 1030 cm^{-1}; MS, *m/z* (relative intensity) 152 (M^+, 6), 134 (1), 94 (5), 80 (100), 79 (33), 73 (35), 67 (12). Anal. Calcd for $C_9H_{12}O_2$: C, 71.02; H, 7.95. Found: C, 71.23; H, 8.24.

2,8-Noradamantanedione (**8**) was prepared in 89% and 55% yield by Jones oxidation of **7** and **5**, respectively, following the procedure described for **6**. However, the crude product was purified by sublimation rather than column chromatography. **8** (pure by ^{13}C NMR): mp 211–213 °C; ^{13}C NMR ($CDCl_3$) δ 209.4 (s, 2 C), 64.0 (d, 1 C), 52.4 (d, 2 C), 45.8 (t, 2 C), 44.5 (t, 1 C), 35.0 (d, 1 C); ^1H NMR ($CDCl_3$) δ 3.17–2.82 (m, 3 H), 2.63–2.11 (m, 7 H, maximum at δ 2.29); IR (KBr) 2943, 2875, 1775, 1730, 1450, 1218, 1054, 873, 798 cm^{-1}; MS, *m/z* (relative intensity) 150 (M^+, 41), 94 (23), 80 (64), 79 (39), 78 (21), 67 (38), 66 (100), 55 (41). Anal. Calcd for $C_9H_{10}O_2$: C, 71.98; H, 6.71. Found: C, 72.05; H, 6.92.

2-*exo*-Noradamantanol (9). A solution of hydroxy ketone **7** (650 mg, 4.3 mmol) and tosylhydrazine (880 mg, 4.7 mmol) in methanol (10 mL) was stirred for 12 h at room temperature. Evaporation of the solvent yielded the crude hydroxy tosylhydrazone **7a**, which was used without purification in the next step.

A 1.9 M solution of diborane in dry THF (3.6 mL) was added to a solution of benzoic acid (1.0 g, 8.2 mmol) in chloroform (10 mL) stirred at 0 °C. After 10 min, a solution of the hydroxy tosylhydrazone **7a** in chloroform (3 mL) was added and the resulting mixture was stirred for an additional hour at 0 °C. Sodium acetate trihydrate (2.7 g, 19.8 mmol) was added afterward and the reaction mixture was stirred overnight at room temperature. Water (30 mL) was then added followed by ether (50 mL). The organic layer was separated, washed with saturated aqueous $NaHCO_3$ solution (5 × 30 mL), and dried ($MgSO_4$). The solvent was evaporated and the crude product was purified by column chromatography on neutral alumina (activity II/III). Elution with pentane–ether (1:0 to 1:1) yielded alcohol **9** (180 mg, 30% based on **7**; ≥98% pure by GC, DEGS, 170 °C). The ^1H NMR and IR spectral data were consistent with those reported[3f] for 2-*exo*-noradamantanol. **9**: ^{13}C NMR ($CDCl_3$) δ 83.7 (d), 46.2 (d), 43.6 (t), 43.4 (d), 41.3 (t), 39.1 (t), 36.3 (d), 35.1 (d), 34.5 (t); MS, *m/z* (relative intensity) 138 (M^+, 5), 120 (22), 92 (20), 91 (25), 79 (100), 78 (45), 67 (36), 66 (28).

2-Noradamantanone (10). Alcohol **9** (170 mg, 1.23 mmol) was oxidized by the procedure described for **6**. The crude product was purified by column chromatography on neutral alumina (activity II/III). Elution with pentane–ether (3:1) yielded ketone **10** (145 mg, 86.7%; ≥98% pure by GC, DEGS, 170 °C), the spectral data of which were in complete agreement with those reported previously.[18]

2-*endo*-Noradamantanol (11) was obtained in 90% yield by $LiAlH_4$ reduction of **10** following the procedure described for 4-brendanol. **11**: ^{13}C NMR ($CDCl_3$) δ 77.2 (d), 43.5 (t), 40.5 (d), 40.0 (d), 38.1 (t), 37.2 (d), 35.9 (d), 33.3 (t), 30.3 (t); ^1H NMR ($CDCl_3$) δ 4.05 (dd, J_1 = 5.8 Hz, J_2 = 3.2 Hz, 1 H), 2.5–1.1 (m, 13 H); IR (KBr) 3280, 2920, 2860, 1455, 1350, 1310, 1295 , 1145, 1100, 1040 cm^{-1}; MS, *m/z* (relative intensity) 138 (M^+, 4), 120 (19), 92 (20), 91 (26), 79 (100), 78 (41), 67 (40), 66 (32).

Acknowledgment. This work was supported by a grant from the Research Council of the Republic of Croatia (SIZ II).

Registry No. **1**, 1521-78-4; **2**, 88685-69-2; **3**, 88685-70-5; **4**, 88703-07-5; **5**, 88685-71-6; **6**, 88685-72-7; **7**, 88685-73-8; **7a**, 88685-74-9; **8**, 88685-75-0; **9**, 18117-75-4; **10**, 17931-67-8; **11**, 18117-74-3; 4-brendanol, 88762-77-0.

Stereodynamics of Substituted Neopentanes

Michael R. Whalon* and C. Hackett Bushweller*[1]

Department of Chemistry, University of Vermont, Burlington, Vermont 05405

Warren G. Anderson

Department of Chemistry, Worcester Polytechnic Institute, Worcester, Massachusetts 01609

Received August 26, 1983

tert-Butyl rotation barriers have been measured in four monosubstituted neopentanes (Me_3CCH_2X, X = Me, Cl, Br, I) by using 270-MHz ^1H dynamic NMR spectroscopy. The barrier depends on X in the order: Me < Cl ~ Br ~ I. As a complement to the experimental DNMR data, Allinger's MM2 molecular mechanics program (1980 force field) was used to calculate optimized equilibrium geometries and *tert*-butyl rotation barriers for the four compounds. The MM2 barriers are compared to previously reported MM1 barriers.

Neopentyl systems have been important in the study of steric effects on the rate of a variety of reactions. Since it has been demonstrated that the rotation barrier about the quaternary carbon–secondary carbon bond in neopentyl[2–4] and related systems [i.e., $Me_2C(CH_2X)_2$, $MeC(CH_2X)_3$, X = Me, halogen][5] is accessible to the ^1H or $^{13}C\{^1H\}$ dynamic nuclear magnetic resonance (DNMR) method, the neopentyl systems constitute simple, experimentally accessible models for the *tert*-butyl rotation process.

(1) Alfred P. Sloan Research Fellow; Camille and Henry Dreyfus Teacher-Scholar.

(2) Bushweller, C. H.; Anderson, W. G. *Tetrahedron Lett.* **1972**, 1811.

(3) Bushweller, C. H.; Hoogasian, S.; Anderson, W. G.; Letendre, L. J. *J. Chem. Soc., Chem. Commun.* **1975**, 152.

(4) Freitag, W.; Schneider, H. *Israel J. Chem.* **1980**, *20*, 153.

(5) Bushweller, C. H.; Whalon, M. R.; Fleischman, S. H.; Rithner, C. D.; Sturges, J. S. *J. Am. Chem. Soc.* **1979**, *101*, 7073. Bushweller, C. H.; Whalon, M. R.; Laurenzi, B. J. *Tetrahedron Lett.* **1981**, *22*, 2945. Whalon, M. R.; Grady, G. L.; McGoff, P.; Domingue, R.; Bushweller, C. H. *Tetrahedron Lett.* **1982**, *23*, 5247.

0022-3263/84/1949-1185$01.50/0

Table I. Me_3C-CH_2-X Chemical Shifts[a] and Coupling Constants[b]

compd	X	temp, K	Me_3C, ppm	CH_2, ppm	X, ppm	$^3J_{HH}$, Hz
1	Me	130[c]	0.89 (9 H)	1.23	0.86	7.5
		98[d]	0.86 (6 H), 0.94 (3 H)	1.23	0.86	7.5
2	Cl	130[c]	1.03 (9 H)	3.33		
		100[d]	1.04 (6 H), 1.07 (3 H)	3.39		
3	Br	140[c]	1.08 (9 H)	3.30		
		105[d]	1.06 (6 H), 1.16 (3 H)	3.35		
4	I	140[c]	1.12 (9 H)	3.18		
		105[d]	1.05 (6 H), 1.27 (3 H)	3.24		

[a] ^1H in ppm, Me_4Si reference. [b] Hz, proton-proton coupling. [c] Fast *tert*-butyl rotation. [d] Slow *tert*-butyl rotation.

In previous communications, we reported *tert*-butyl rotation barriers ($\Delta G^{\ddagger}$) for **1** (4.9 ± 0.5 kcal/mol at 92 K),[2] **3** (6.0 ± 0.2 kcal/mol at 104 K),[3] and **4** (5.9 ± 0.2 kcal/mol at 107 K).[3] In these studies, we employed the ^1H DNMR method albeit at a low operating frequency (60 MHz). A decoalescence was not observed for **2** and the low temperature spectra of **1** were ill defined.[2] It is interesting to note that a decoalescence of the methyl $^{13}C\{^1H\}$ NMR resonances of **2** allowed an estimate of the *tert*-butyl rotation barrier ($\Delta G^{\ddagger}$ = 6.5 ± 0.2 kcal/mol at 150 K).[4]

$$Me_3CCH_2X$$

1, X = Me; **2**, X = Cl; **3**, X = Br; **4**, X = I

This paper reports the results of ^1H DNMR studies (270 MHz) of the neopentyl systems **1–4**. The spectrum of the *tert*-butyl group of **2** at 270 MHz does in fact decoalesce revealing a small chemical shift difference between methyls gauche and anti to chlorine and, upon comparison to **3** and **4**, an interesting trend in the anisotropies of the carbon–halogen bonds. In addition, a better resolved low-temperature spectrum of **1** is obtained at 270 MHz. As a complement to the ^1H DNMR data, we used Allinger's MM2 molecular mechanics program (1980 force field) to calculate the optimized equilibrium geometries and *tert*-butyl rotation barriers for **1–4**.[6] These MM2 barriers for **1–4** are compared to previously reported MM1 barriers.[4]

Results and Discussion

^1H DNMR spectral data for **1–4** (2% v/v in $CBrF_3$, 270 MHz) under conditions of fast DNMR interchange (above 120 K) and slow exchange (98 to 105 K) appear in Table I. In each case, the spectrum of the *tert*-butyl group decoalesces at low temperatures to reveal two distinct methyl singlets in a 2:1 ratio while the methylene signal undergoes no decoalescence. This spectral behavior is consistent with slowing 3-fold *tert*-butyl rotation. The methyl *singlets* reveal rapid rotation of individual methyl groups even at 100 K.

The ^1H spectrum of **1** (Figure 1) consists of two subspectra due to the *tert*-butyl and ethyl groups. At temperatures above 130 K, the spectrum of the *tert*-butyl group is a singlet. At lower temperatures, the *tert*-butyl signal decoalesces and is separated at 98 K into two singlets at δ 0.86 (6 H) and 0.94 (3 H). The A_2C_3 spectrum (δ_A 1.23, δ_C 0.86, $^3J_{AC}$ = 7.5 Hz) for the ethyl group remains unchanged except for broadening (shorter T_2 values) due to

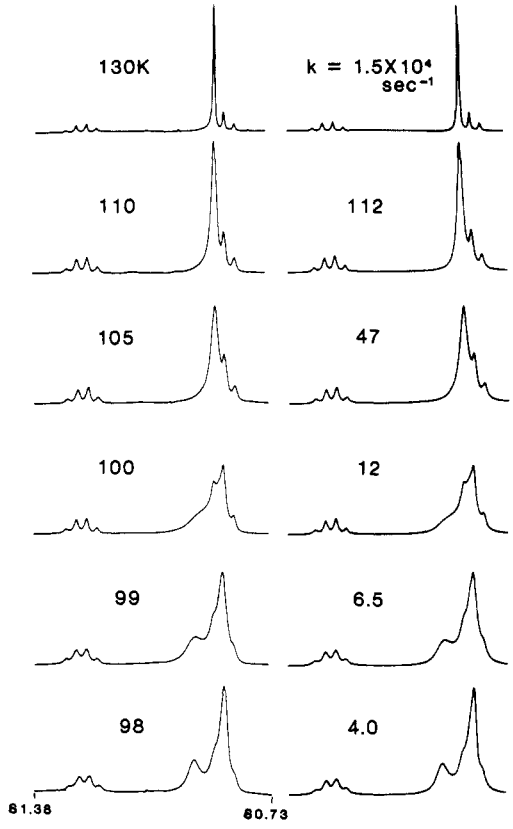

Figure 1. Experimental ^1H DNMR spectra (270 MHz) of Me_3C-CH_2Me (**1**, 2% v/v in $CBrF_3$) in the left column and theoretical DNMR simulations in the right column. *k* is the first order rate constant for the conversion of one *tert*-butyl rotamer to one other rotamer.

increasing viscosity at progressively lower temperatures. This spectral behavior is consistent with slowing *tert*-butyl rotation on the DNMR time scale and the spectrum at 98 K is consistent with a staggered equilibrium geometry for **1** as illustrated in structure **5** (C_s symmetry). The *tert*-butyl methyl groups gauche to the C4 carbon in **5** will, of course, have identical NMR chemical shifts. The *tert*-butyl methyl group anti to C4 is in an environment which is different from the two gauche methyls. In principle, the *tert*-butyl methyl groups should give rise to two different signals in the slow exchange DNMR spectrum in a 2:1 (gauche methyls:anti methyl) ratio, as observed. The methylene protons in **5** are enantiotopic and will have the same NMR chemical shifts in the achiral solvent $CBrF_3$. No decoalescence of the methylene protons resonance should be observed due to slowing 3-fold *tert*-butyl rotation, as observed.

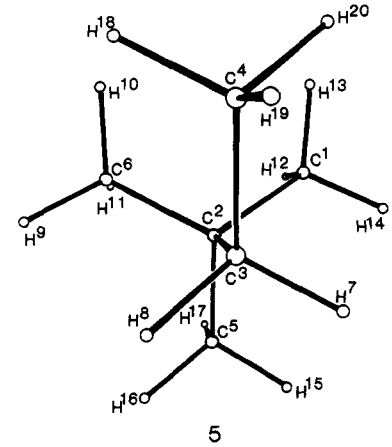

5

(6) Allinger, N. L.; Yuh, Y. J. "Quantum Chemistry Program Exchange"; Indiana University: Bloomington, IN, 1980; Program No. 395.

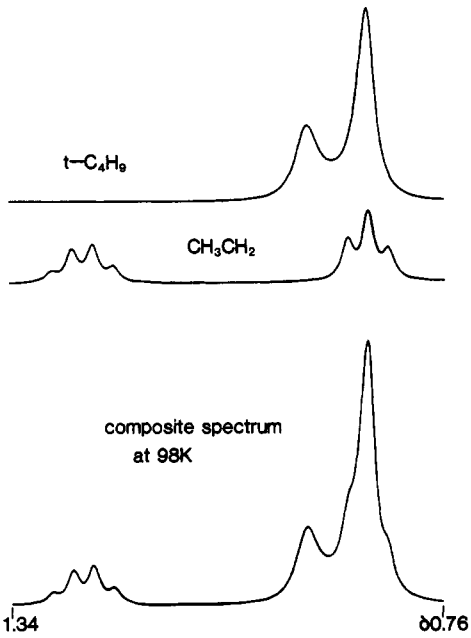

Figure 2. Theoretical decomposition of the ^{1}H DNMR spectrum (270 MHz) of Me_3C-CH_2Me at 98 K.

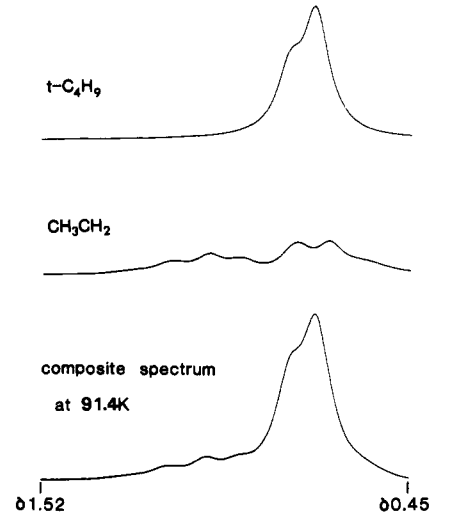

Figure 3. Theoretical decomposition of the ^{1}H DNMR spectrum (60 MHz) of Me_3C-CH_2Me at 91.4 K.

The theoretically simulated *composite* spectrum of **1** at 98 K and the two subspectra are illustrated in Figure 2.[7] The top subspectrum (Figure 2) shows the two singlets due to the *tert*-butyl methyl groups at 98 K. The middle subspectrum displays the A_2C_3 spectrum for the ethyl group. The bottom composite spectrum results from the addition of the upper two subspectra. Comparison of the 270-MHz ^{1}H DNMR spectrum of **1** at 98 K (Figure 2) with a composite simulation and decomposition of the previously obtained 60-MHz ^{1}H DNMR spectrum at 91.4 K (Figure 3)[2] reveals considerably more detail in the higher field spectrum. Not only are the methyl resonances better resolved in the higher field spectrum but also the methylene signal is removed from the vicinity of the exchanging *tert*-butyl resonances.

As shown in Figure 1, even at 98 K, the slow exchange limit for *tert*-butyl rotation in **1** is not achieved. A rate constant of 4 s^{-1} is required to adequately fit the spectrum. However, line shape analysis reveals the barrier (ΔG^*) to *tert*-butyl rotation in **1** to be 5.2 ± 0.2 kcal/mol at 100 K in good agreement with our previously reported barrier of 4.9 ± 0.5 kcal/mol at 92 K obtained at 60 MHz.[2]

The ^{1}H NMR spectrum (270 MHz) of neopentyl chloride (**2**, 2% v/v in $CBrF_3$) at 130 K consists of two sharp singlets at δ 1.03 (t-C_4H_9) and 3.33 (CH_2Cl). Below 110 K, the *tert*-butyl resonance broadens asymmetrically, decoalesces, and, at 100 K, is sharpened into two closely spaced singlets at δ 1.04 (6 H) and 1.07 (3 H). The CH_2Cl signal undergoes no change except for some viscosity (T_2) broadening at very low temperatures. The observation of the two *tert*-butyl singlets at 100 K is consistent with slow *tert*-butyl rotation in **2** and the staggered molecular conformation illustrated in **6** (C_s symmetry). Although a

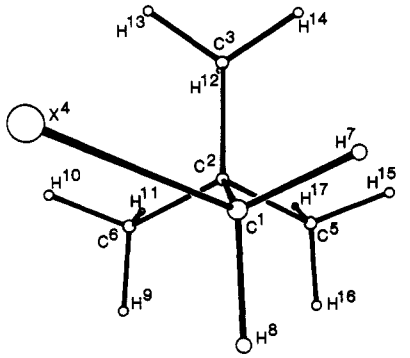

6

decoalescence of the $^{13}C\{^1H\}$ DNMR spectrum of **2** attributable to *tert*-butyl rotation has been observed,[4] this work represents the first observation of a decoalescence of the ^{1}H DNMR spectrum for **2**. A previous attempt in our laboratory at 60 MHz failed to resolve the small chemical shift difference (0.03 ppm at 100 K) between the gauche and anti *tert*-butylmethyl signals of **2**. The methylene protons singlet undergoes no decoalescence consistent with symmetry considerations (see **6**). From complete line shape analysis, the barrier (ΔG^*) to *tert*-butyl rotation for **2** is calculated to be 5.9 ± 0.2 kcal/mol at 107 K.

Neopentyl bromide (**3**) and neopentyl iodide (**4**) as 2% v/v solutions in $CBrF_3$ also display ^{1}H DNMR behavior completely analogous to **2**, although the ^{1}H chemical shift difference between gauche and anti methyls at slow exchange progressively increases from **2** to **3** to **4** (Table I). The "coalescence" temperatures for **3** and **4** are 121 ± 3 K and 124 ± 3 K, respectively. Barriers to *tert*-butyl rotation in **3** (ΔG^* = 6.0 ± 0.2 kcal/mol at 117 K) and **4** (ΔG^* = 6.0 ± 0.2 kcal/mol at 125 K) as determined from simulation of the 270-MHz spectra confirm within experimental error our previously reported barriers determined at 60 MHz (ΔG^* = 6.0 ± 0.2 kcal/mol at 104 K for **3**, ΔG^* = 5.9 ± 0.2 kcal/mol at 107 K for **4**).[3] A previously reported *tert*-butyl rotation barrier for **2** of 6.5 ± 0.2 kcal/mol at 150 K determined from $^{13}C\{^1H\}$ DNMR spectra appears to be slightly at variance with our value (5.9 ± 0.2 kcal/mol). Indeed, our value seems to reflect better the general trend that chlorine is somewhat less effective at restricting rotation than bromine.[8]

(7) The DNMR line shape simulation program used is a substantially revised version of DNMR3 written by Kleier, D. A.; Binsch, G. "Quantum Chemistry Program Exchange"; Indiana University: Bloomington, IN; Program No. 165. Our local revisions are described in Bushweller, C. H.; Bhat, G.; Letendre, L. J.; Brunelle, J. A.; Bilofsky, H.; Ruben, H.; Templeton, D. H.; Zalkin, A. *J. Am. Chem. Soc.* **1975**, *97*, 65.

(8) (a) Anderson, J. E.; Pearson, H. *J. Chem. Soc. B* **1971**, 1209. Anderson, J. E.; Pearson, H. *J. Chem. Soc., Chem. Commun.* **1971**, 871. (b) Hawkins, B. L.; Bremser, W.; Borcic, S.; Roberts, J. D. *J. Am. Chem. Soc.* **1971**, *93*, 4472.

At this point, it is appropriate to comment on the fact that our discussion above focuses on the $\Delta G^{\ddagger}$ values for *tert*-butyl rotation. We have indeed determined $\Delta H^{\ddagger}$ and $\Delta S^{\ddagger}$ values from the 270-MHz spectra for **1** (5.6 ± 0.4 kcal/mol, 4.2 ± 2.0 cal/deg mol), **2** (6.2 ± 0.4 kcal/mol, 2.9 ± 2.0 cal/deg mol), **3** (5.8 ± 0.4 kcal/mol, −1.5 ± 2.0 cal/deg mol), and **4** (6.7 ± 0.4 kcal/mol, 5.5 ± 2.0 cal/deg mol). In simulating the spectra, we assumed the effective T_2 value for the *tert*-butyl protons is identical with that of the nonexchanging methylene protons. In light of this assumption and the error in sample temperature measurement (±3 K), the $\Delta H^{\ddagger}$ and $\Delta S^{\ddagger}$ values should be viewed with caution. The 60-MHz spectra of **1**, **3**, and **4** were recorded by using a custom-built probe which provided very accurate temperature measurement at the sample (±0.2 K, see Experimental Section). However, the chemical shift separations in Hz for **1** are miniscule at 60 MHz and DNMR decoalescence occurs over a very short temperature range. This precludes the extraction of accurate $\Delta H^{\ddagger}$ and $\Delta S^{\ddagger}$ values. Compound **2** showed no decoalescence at 60 MHz. The 60-MHz $\Delta H^{\ddagger}$ and $\Delta S^{\ddagger}$ values for **3** (6.0 ± 0.2 kcal/mol, 0 ± 0.5 cal/mol deg) and **4** (5.9 ± 0.2 kcal/mol, 0 ± 0.5 cal/mol deg) might be considered to be more accurate than the 270-MHz values. In any event, it is well established that the $\Delta G^{\ddagger}$ values are less subject to the systematic errors which can plague $\Delta H^{\ddagger}$ and $\Delta S^{\ddagger}$ values and we choose to use $\Delta G^{\ddagger}$ values for comparison.

Some interesting trends in proton NMR chemical shifts are observed for **2**–**4** (Table I). In the slow exchange spectrum of the *tert*-butyl group of each compound, the methyl group located anti to halogen consistently resonates at lower field than the methyl groups gauche to halogen. This has been noted previously for **3**[3] and **4**[3] and is also true for **2**. While the chemical shifts of methyl groups gauche to halogen seem to be insensitive to halogen in **2**–**4** (Table I), the anti methyl group experiences increasing deshielding in progressing from chlorine to bromine to iodine. Any differential inductive effect due to halogen in **2**–**4** must traverse four bonds and must be considered inconsequential. In any event, the chemical shift trend is in the wrong direction. It is noteworthy that, as in other cases,[9] there seems to be an inverse correlation of the deshielding of the anti methyl signal with halogen electronegativity. Chlorine, the most electronegative halogen in the series **2**–**4**, gives rise to the smallest chemical shift difference between the gauche and anti methyl groups. The unique combination of shielding factors responsible for the observed trend that gauche methyl signals are found at higher field than anti remains unclear. A McConnell model[10] of the shielding due to the diamagnetic anisotropy of the C–X bond predicts the gauche methyl to be downfield from the anti methyl signal, in contrast with the observed data. Electron densities on the various protons of **2** obtained from MNDO[11] calculations indicate that the time-averaged electron density for the protons on a rapidly rotating methyl group gauche to chlorine is lower than for the protons on a methyl group anti to chlorine. This would indicate a deshielding of the protons on the gauche methyl group with respect to the anti methyl protons again in contrast with the data. It is apparent that neither the shift to lower field of the anti methyl resonance with decreasing electronegativity nor the relative high-field position of the gauche methyl signal can be rationalized

Table II. MM2 Optimized Geometry Parameters

compd	C2–C3[a] length	C1–C2–C3[a] angle	C3–C2–C5[a] angle	C3–C2–C6[a] angle	C2–C3–C4[a] angle	C4–C3–C2–C5[a] dihedral angle[c]	C4–C3–C2–C1[a] dihedral angle[c]	C4–C3–C2–C6[a] dihedral angle[c]
1 staggered	1.5478	111.127	108.341	111.145	116.152	−179.747[c]	61.252	−60.728
eclipsed[b]	1.5543	113.809	109.511	109.411	117.210	120.910	0	−120.794
	C1–C2[d] length	C1–C2–C3[d] angle	C1–C2–C5[d] angle	C1–C2–C6[d] angle	X–C1–C2[d] angle	X–C1–C2–C5[d] dihedral angle[c]	X–C1–C2–C3[d] dihedral angle[c]	X–C1–C2–C6[d] dihedral angle[c]
2 staggered	1.5443	111.151	107.872	111.284	114.296	−179.266[c]	62.093	−60.579
eclipsed[b]	1.5518	114.611	109.143	109.073	116.298	121.049	0	−120.900
3 staggered	1.5452	111.644	107.405	111.648	114.922	−179.918[c]	61.791	−61.622
eclipsed[b]	1.5528	115.579	108.891	108.806	116.986	121.269	0	−121.085
4 staggered	1.5445	111.459	107.571	111.643	117.008	−179.093[c]	62.625	−60.754
eclipsed[b]	1.5519	115.133	109.084	109.017	119.406	121.072	0	−120.936

[a] For **1**, see structure **5** for assignments of atoms. [b] Eclipsed geometries for **1**–**4** were calculated by using the restricted motion method by fixing dihedral angle C4–C3–C2–C1 in **1** and X–C1–C2–C3 in **2**–**4** at 0°. [c] When viewing structure **5** through C3 toward C2 a negative sign indicates that the specified atom (C1, C5, or C6) is counterclockwise from C4. In structure **6** looking from C1 toward C2 the negative sign indicates that the specified atom (C3, C5, or C6) is counterclockwise from X. [d] For **2**–**4**, see structures **6** (staggered) and **7** (eclipsed) for assignment of atoms.

(9) Fort, R. C., Jr.; von R. Schleyer, P. *J. Org. Chem.* **1965**, *30*, 789.
(10) McConnell, H. M. *J. Chem. Phys.* **1957**, *27*, 226.
(11) Thiel, W. "Quantum Chemistry Program Exchange"; Indiana University: Bloomington, IN, 1978; Program No. 353.

Table III. Me_3C-CH_2X Barriers to *tert*-Butyl Rotation in kcal/mol

compd	X	MM1[a]	MM2[b]	experimental barriers ($\Delta G^{\ddagger}$) this study	literature
1	Me	3.85	3.86	5.2 ± 0.2 (100 K)	4.9 ± 0.5 (92 K)[c]
2	Cl	5.10	5.78	5.9 ± 0.2 (107 K)	6.5 ± 0.2 (150 K)[a]
3	Br	5.05	7.54	6.0 ± 0.2 (117 K)	6.0 ± 0.2 (105 K)[d]
4	I	5.45	5.18	6.0 ± 0.2 (125 K)	5.9 ± 0.2 (107 K)[d]

[a] Reference 4. [b] Reference 6. [c] Reference 2. [d] Reference 3.

on the basis of these simple models. Other factors must play roles in the determination of chemical shift.

Optimized equilibrium molecular geometries and optimized transition states for *tert*-butyl rotation for **1–4** were calculated in our laboratory by using the molecular mechanics method (Table II, Allinger's 1980 MM2 force field).[6] *tert*-Butyl rotation barrier calculations for **1–4** were done using the dihedral angle driver method rather than the restricted motion method (Table III).[6] Some previously reported MM1 barriers are included in Table III for comparison. MM2 parameters for iodine are not yet refined and the results for **4** must be viewed with caution.[6]

Optimized MM2 calculations for the equilibrium geometries of **1–4** reveal interesting trends (Table II). Dihedral angles (C4–C3–C2–C5 in **5** and C5–C2–C1–X in **6**) defining the position of the anti *tert*-butyl methyl group with respect to the X substituent in **1–4** are very nearly 180° in each case (−179.75° in **1**, −179.27° in **2**, −179.92° in **3**, and −179.09° in **4**, see Table II) suggesting that the staggered equilibrium geometries for **1–4** indeed possess essentially perfect C_s symmetry. The data further suggest that van der Waals interactions in **1–4** are optimized primarily at the expense of bond angle bending and to a lesser degree by bond stretching. In each case (**1–4**), the central bond length (C2–C3 in **5** and C1–C2 in **6**) is increased beyond the idealized carbon–carbon bond length of 1.54 Å and bond angles are expanded beyond the tetrahedral angle of 109.5°. Selected parameters from the optimized MM2 geometries of **1–4** are listed in Table II. The most dramatic bond angle opening is the C2–C1–X bond angle in **6** and C2–C3–C4 bond angle in **5** (Table II) which increases to over 114° in all four cases. It is also noteworthy that in the staggered equilibrium geometry (**5** or **6**), the bond angles defined by the two gauche methyl groups (C1–C2–C3 and C3–C2–C6 in **5** and C1–C2–C3 and C1–C2–C6 in **6**) have increased to about 111° while the analogous bond angle for the anti methyl group (C3–C2–C5 in **5** and C1–C2–C5 in **6**) is slightly compressed from the standard value of 109.5°. As X rotates toward C3 in **6** or C4 rotates toward C1 in **5**, approaching an eclipsed transition state (e.g., **7**), MM2 calculations suggest that the C1–C2–C6 bond angle in **6** (C3–C2–C6 in **5**) begins to relax back to a relatively unstrained value while the C2–C1–X bond angle in **6** (C2–C3–C4 in **5**) increases by an additional 1 to 2° and the C1–C2–C3 bond angle also increases (Table II). It is apparent that several kinds of reorientation occur during the *tert*-butyl rotation itinerary.

The MM2 force field underestimates the barriers in **1** and **4** while overestimating the barrier in **3** (Table III). The MM2 barrier for **2** agrees well with the experimental $\Delta G^{\ddagger}$ value. A progressive underestimation of barriers to carbon–carbon bond rotation by MM2 in progressively more sterically congested hydrocarbons has been noted

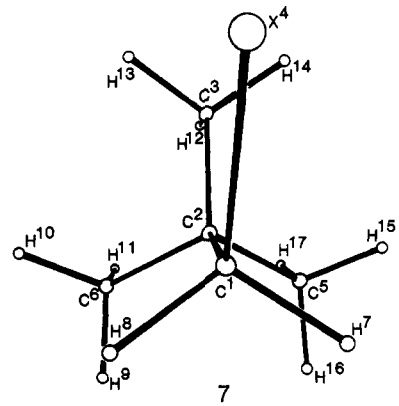

7

previously.[12] A method of "correcting" for calculated barriers has been proposed.[12] For hydrocarbons with transition states for rotation involving methyl–methyl eclipsing, i.e., the conversion of *n*-butane from one gauche form directly to the other gauche form or the conversion of 2,3-dimethylbutane from the anti to the gauche form, MM2 predicts barriers to carbon–carbon bond rotation which are lower than the experimental barrier by approximately 1.2 kcal/mol per methyl–methyl eclipsing.[12] Since there is only one such interaction in the transition state for **1**, it seems appropriate to add 1.2 kcal/mol to the MM2 barrier (3.86 kcal/mol) to obtain a "corrected" MM2 barrier of 5.06 kcal/mol in good agreement with the experimentally observed barrier of 5.2 kcal/mol.

In order to make a more wide ranging assessment of trends between the MM2 calculated rotation barriers and experimental barriers, the MM2 barriers for several relevant compounds can be compared with experiment (Table IV). The data indicate that even after correcting the MM2 barriers for methyl–methyl eclipsing, the agreement with experiment is in general only approximate. However, it may also be reasonable to suggest rotation barrier "corrections" for compounds such as **2–4**. For example, in 2-chloro-2,3-dimethylbutane (**16**, Table IV), consider conversion of the gauche form to the anti form via rotation about the C2–C3 bond involving transition state **16a** (Table IV, $\Delta G^{\ddagger}_{exp}$ = 7.4 kcal/mol;[17] $\Delta H^{\ddagger}_{MM2}$ = 5.73 kcal/mol).[15] The transition state **16a** involves a methyl–chlorine, a methyl–methyl, and a methyl–hydrogen eclipsing interaction. A correction of +1.4 kcal/mol for each methyl–methyl interaction has been suggested for a structurally similar hydrocarbon, i.e., 2,2,3-trimethylbutane.[12] Assuming a methyl–methyl eclipsing correction of 1.4 kcal/mol, and assuming no correction for a methyl–hydrogen interaction, then the methyl–chlorine correction must be approximately 0.3 kcal/mol in order to produce agreement with the observed barrier for the gauche to anti process via **16a**. Indeed, for the other chloroalkanes in Table IV (**9**, **13**), each MM2 prediction remains approximately 0.3 kcal/mol shy of the experimental barrier to carbon–carbon bond rotation if we employ the 1.4 kcal/mol correction for each methyl–methyl eclipsing. Furthermore, we note that in transition state

(12) Osawa, E.; Shirahama, H.; Matsumoto, T. *J. Am. Chem. Soc.* **1979**, *101*, 4824.
(13) Anderson, J. E.; Pearson, H. *J. Chem. Soc., Chem. Commun.* **1972**, 908.
(14) Bushweller, C. H.; Anderson, W. G.; Goldberg, M. J.; Gabriel, M. W.; Gilliom, L. R.; Mislow, K. *J. Org. Chem.* **1980**, *45*, 3880.
(15) Meyer, A. Y.; Allinger, N. L.; Yuh, Y. *Israel J. Chem.* **1980**, *20*, 57.
(16) Anderson, J. E.; Doecke, C. W.; Pearson, H. *J. Chem. Soc., Perkin Trans. 2* **1976**, 336.
(17) Anderson, J. E.; Pearson, H. *J. Chem. Soc. Perkin Trans. 2* **1973**, 960.

Table IV. Barriers to Rotation in Substituted Ethanes

	compd	MM2 barrier[a]	corrected[b] MM2 barrier	experimental barrier $\Delta G^{\ddagger}$	exp - corrected MM2[c] difference
8	Me_3C-$CHMe_2$	4.1[d]	6.9[d]	6.9[e]-6.97[f]	0
9	Me_3C-CHMeCl	6.07	7.47	7.7[g]-7.87[f]	0.35
10	Me_3C-CHMeBr	7.80		7.8[g]	
11	Me_3C-CHMeI	5.49	6.89		
12	Me_3C-CMe_3	5.3[d]	9.8[d]	8.8[h]	−1.0[i]
13	Me_3C-CMe_2Cl	7.05[j]	10.04	10.43[k]	0.3
14	Me_3C-CMe_2Br	8.99[j]		10.73[k]	
15	Me_3C-CMe_2I	6.74		11.14[k]	
16	Me_2HC-CMe_2Cl				
a	Cl/Me eclipsed	5.73[j]	7.13	7.4[l]	0.27
b	Cl/H eclipsed	5.34[j]	8.14	8.2[l]	0

[a] Some MM2 calculated barriers have appeared in the literature. All MM2 calculations were verified in our laboratory (ref 6). [b] A corrected MM2 barrier using a correction of +1.40 kcal/mol for each Me/Me eclipsing in the transition states of **8-11** and **16a-16b** and a correction of +1.50 kcal/mole for each Me/Me eclipsing in the transition states of **12-15** (ref 12). [c] The difference between the experimental barrier and the corrected MM2 barrier using the correction outlined in *b*. [d] Reference 12. [e] Reference 2. [f] Reference 13. [g] Reference 4. [h] The barrier for **12** has been estimated by extrapolation from experimentally determined barriers for two similar systems (2,2,3,3-tetramethylpentane and 3,3,4,4-tetramethylhexane, ref 14). [i] The extrapolated barrier for **12** is overestimated by 1.0 kcal/mol by using the MM2 computed barrier for **12** plus the recommended (ref 12) correction factor of +1.5 kcal/mol for each Me/Me eclipsing in the transition state for **12**. [j] Reference 15. [k] Reference 16. [l] Reference 17.

16b for the gauche to gauche process in **16** (Table IV), there are two methyl–methyl and one hydrogen–chlorine eclipsing interactions. Applying the hydrocarbon correction of 2 × 1.4 kcal/mol to the MM2 barrier results in an excellent approximation (8.14 kcal/mol) to the experimentally observed barrier (8.2 kcal/mol). We conclude that a correction of 0.3 kcal/mol must be added to MM2 calculated barriers for each chlorine–methyl eclipsing in the rotation transition state, while a chlorine–hydrogen eclipsing needs no correction. Application of this "correction" term to the MM2 calculated barrier for **2** gives a "corrected" barrier of 6.08 kcal/mol in good agreement with the experimental barrier (5.9 kcal/mol).

A similar approach might be applied to MM2 barrier corrections for the bromoalkanes **3** (Table III), **10**, and **14** (Table IV). However, the discrepancies between the experimental barriers ($\Delta G^{\ddagger}$) for **3**, **10**, and **14** (6.0, 7.8, and 10.7 kcal/mol) and the MM2 barriers (7.5, 7.8, and 9.0 kcal/mol) show much less consistency than the chloroalkane series. We hesitate to suggest any MM2 barrier corrections for pairwise substituent interactions in the bromoalkanes until more data is available. The iodoalkanes must be considered in the same light.

In light of the corrections which must be applied to the MM2 barrier calculations to obtain good agreement with experiment and the variation in the "uncorrected" MM2 results, particularly in the case of the bromoalkanes, the MM1 force field gives a better reflection of the observed experimental barriers for **1–4**. Although the MM1 calculated barriers are consistently about 1 kcal/mol below the experimental barriers, the barriers calculated by MM1 (Table III) better reflect the observed barrier *trend*.

Experimental Section

NMR spectra were run on a Bruker HX 270 pulsed Fourier transform NMR system at the Northeast Regional NSF–NMR Facility at Yale University. The accuracy of the probe temperatue measurement was established by comparison of previously obtained 60-MHz rate data for compounds **3** and **4** where probe temperatures were known to a high degree of accuracy (±0.2 K)[18] to data obtained on the Yale instrument for the same compounds. At very low temperatures, temperature measurement on the HX270 is accurate to ±3 K. All NMR samples were prepared in precision NMR tubes on a vacuum line, degassed three times, and the NMR tubes sealed.

2,2-Dimethylbutane (99.9+%) was purchased from Chemical Samples Company and was used without further purification.

Neopentyl chloride and neopentyl bromide were purchased from Fairfield Chemical Company, Inc. Careful GLPC analysis using a 5 ft × 3/8 in. FFAP preparative column at 343 K and a flow rate of 20 mL/min indicated no impurities present. ^1H NMR: see Table I.

Neopentyl Iodide. Neopentyl alcohol (Aldrich, 99% pure) was converted to the tosylate according to a published procedure.[19] The iodide was prepared by treating 23.2 g of neopentyl tosylate (0.096 mol) with 33.2 g (0.2 mol) of potassium iodide in 150 mL of dimethylformamide at 373 K for 8 h. The mixture was then placed in a separatory funnel with 150 mL of water and 150 mL of ether. After shaking, the aqueous layer was discarded. The ether layer was washed five times with 75-mL portions of water to remove the remaining dimethylformamide and dried over $MgSO_4$. The ether was removed under vacuum and the product purified by GLPC using a 5 ft × 3/8 in. preparative FFAP column at 343 K with a flow rate of 30 mL/min. ^1H NMR: see Table I.

Acknowledgment. We are grateful to the National Science Foundation for support (Grant No. CHE78-21161, and CHE80-24931). We also acknowledge National Science Foundation Grant No. CHE79-16210 from the Chemistry Division in support of the Northeast Regional NSF–NMR Facility at Yale University.

Registry No. **1**, 75-83-2; **2**, 753-89-9; **3**, 630-17-1; **4**, 15501-33-4; **8**, 464-06-2; **9**, 5750-00-5; **10**, 26356-06-9; **11**, 24556-56-7; **12**, 594-82-1; **13**, 918-07-0; **14**, 16468-75-0; **15**, 27705-19-7; **16**, 594-57-0; neopentyl alcohol, 75-84-3; neopentyl tosylate, 2346-07-8; potassium iodide, 7681-11-0.

(18) Jensen, F. R.; Smith, L. A.; Bushweller, C. H.; Beck, B. H. *Rev. Sci. Instrum.* **1972**, *43*, 894.
(19) Fieser, L.; Fieser, M. "Reagents for Organic Synthesis", New York, 1967; p 1180.